

Real-time physical data acquisition through a remote sensing platform on a polar lake

Ben Palethorpe¹, Barrie Hayes-Gill¹, John Crowe¹, Mark Sumner¹, Neil Crout², Malcom Foster¹, Tim Reid², Steve Benford³, Chris Greenhalgh³, and Johanna Laybourn-Parry^{2*}

¹School of Electrical and Electronic Engineering, University of Nottingham, University Park, Nottingham, NG7 2RD, United Kingdom

²School of Biosciences, University of Nottingham, University Park, Nottingham, NG7 2RD, United Kingdom

³School of Computer Science and Information Technology, University of Nottingham, Jubilee Campus, Wollaton Road, Nottingham, NG8 1BB, United Kingdom

Abstract

We describe the design and installation of environmental monitoring equipment on a large freshwater Antarctic lake (Crooked Lake, 68°37'S, 78°23'E). The system recorded ice thickness and photosynthetically active radiation (PAR), ultraviolet (UVB) radiation, and temperature at a range of depths in the water column. The data were accessed remotely at Davis Station (15 km distant) by telemetry. The remote sensing platform produced continuous quasi real-time data, enabling the development of accurate detailed models, e.g., ice heat budget models during seasonal melt out. The prototype system has the capacity for the addition of further instrumentation, for example, fluorimeters. Here we present an illustrative preliminary data set derived during the summer immediately prior to ice-cover break up and after winter redeployment of the platform.

Polar lakes are remote and in climatically challenging environments. As such, they impose major logistic constraints in terms of data acquisition. In many cases they can only be accessed during summer. From a scientific perspective, they are important because they are in latitudes that are experiencing the greatest effects of global warming. However, there are regional and short-term temporal differences in climate change. For example, there are warming trends across parts of the Arctic whereas other areas are cooling (Chapman and Walsh 1993). In Antarctica, the McMurdo Dry Valleys have been the focus of considerable climate study (Doran et al. 2002). There is clear evidence of recent warming that has resulted in increased water levels in the lakes (Webster et al. 1996; Lyons et al. 1997). However, more recent data suggest a phase of cooling in the Dry Valleys, which has impacted primary productivity in the lakes (Doran et al. 2002). Temporal variation in the thickness and optical properties of polar lake ice covers can have profound effects on the process of photo-

synthesis in the water column, and on carbon cycling (Fritsen and Prisco 1999), and numerous models exist for modeling the necessary ice thermodynamics through the parameterization of heat and radiation fluxes (e.g., Fang and Stefan 1996; Launiainen and Cheng 1998; Peeters et al. 2002). These are generally driven by atmospheric variables such as air temperature, wind speed, and radiation, with outputs including ice thickness and ice temperature, but it is unusual to acquire data sets with sufficient temporal resolution for verifying the evolution of such models. There is, therefore, a need for detailed real-time data on the nature of the ice and the light climate in the underlying water column.

Antarctic lakes are delicate, oligotrophic systems that appear to respond rapidly to short-term climate change, and this is manifested in significant interannual variation in productivity and biomass (Roberts et al. 2000; Marshall and Laybourn-Parry 2002). Antarctic lakes possess truncated food webs with low species diversity. In effect, they are dominated by the microbial loop (Laybourn-Parry 1997), and as such, offer systems in which to study microbial plankton dynamics in the absence of top-down controls. For example, such systems can be modeled by considering simple carbon flows between species, giving rise to patterns and oscillations similar to those that occur in larger-scale population dynamics (e.g., Steele and Henderson 1981; Edwards and Brindley 1999). But long-term plankton population data are rare and difficult to measure, particularly

*Corresponding author

Acknowledgments

This work was funded by the Engineering and Physical Sciences Research Council (UK) as part of the E-science program and the Australian Antarctic Science Advisory Committee grant held by J-LP and SB. The authors are grateful for assistance in the field from colleagues at Davis Station, Australian Antarctic Territory.

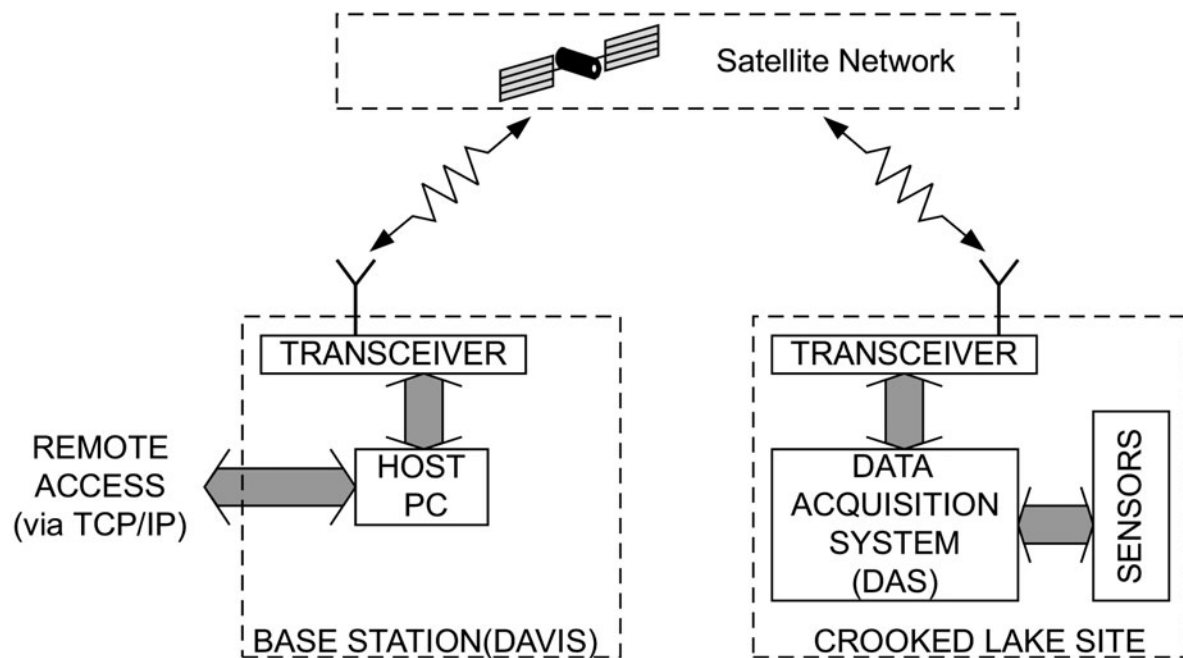


Fig. 1. Overview of entire remote sensing system

in environments like Antarctica. So whereas the database on polar limnology is increasing, there is a pressing need for more detailed, continuous limnological data, that together with experimental data, will enable environmental modelers to develop models demonstrating how polar lakes function, and how they will respond to environmental change.

Remote sensing technology, particularly satellite imagery, has been widely applied in oceanography worldwide, as any student oceanography textbook illustrates (e.g., Sverdrup et al. 2003). The application of ground-based remote sensing technology to lacustrine environments has been less well-exploited, but has enormous potential, particularly in remote locations. To gain a more detailed picture of the physical characteristics of a large freshwater Antarctic lake and enable verification of biological and physical models, we designed a remote sensing platform from which we are able to access data collected every 5 min by satellite telephone link. While the system is currently measuring physical parameters, it has the capacity to accommodate instrumentation capable of measuring biological parameters, e.g., fluorimeters for measuring chlorophyll *a* concentrations. Here we describe the design, installation, and data acquisition from that platform. One of the major considerations was to produce an affordable and reliable ensemble of equipment.

Materials and procedures

System overview—The platform was fixed to the ice surface of Crooked Lake at a point where the water depth was 60 m. Crooked Lake is an ultra-oligotrophic freshwater lake situ-

ated in the Vestfold Hills, a coastal oasis in eastern Antarctica at 68°S, 78°E. It has an area of 9 km² and a maximum depth of 160 m. The remote-sensing system is completely autonomous with battery power charged via solar panels. The platform is comprised of a data acquisition system (DAS), sensors (temperature, UVB radiation, PAR, wind speed, and ice thickness) and a radio transceiver (Fig. 1). All of the sensors are off-the-shelf equipment, regularly used by limnologists in the field with some sensors requiring additional circuitry for signal conditioning. The components and sensors were chosen to withstand low winter temperatures down to -40°C and katabatic winds up to 200 km h⁻¹. Another major factor was budget, the aim being to produce a reliable low-cost system.

Instrumentation—The data acquisition system (DAS), telemetry hardware, and power supply were mounted directly to a welded steel frame bolted to a wooden base. PAR sensors (LI-COR LI-192SA) were run by cable away from the platform across the ice, through holes drilled in the ice and suspended at 3 m, 5 m, 10 m, and 20 m immediately under the ice on individual frames. They were staggered laterally to avoid shading. A reference PAR sensor (LI-COR LI-190SA) was located on the platform at the surface. Two UVB sensors (Skye Instruments SKU-430 UVB) were deployed, one on the platform as a reference for surface values and the other in the water column at 3 m on a frame. Temperature probes (Campbell Scientific 107 temperature probes) were deployed in the water column at 3 m and 5 m. Ice thickness was measured with an upward directed SONAR altimeter, and a wind monitor was positioned

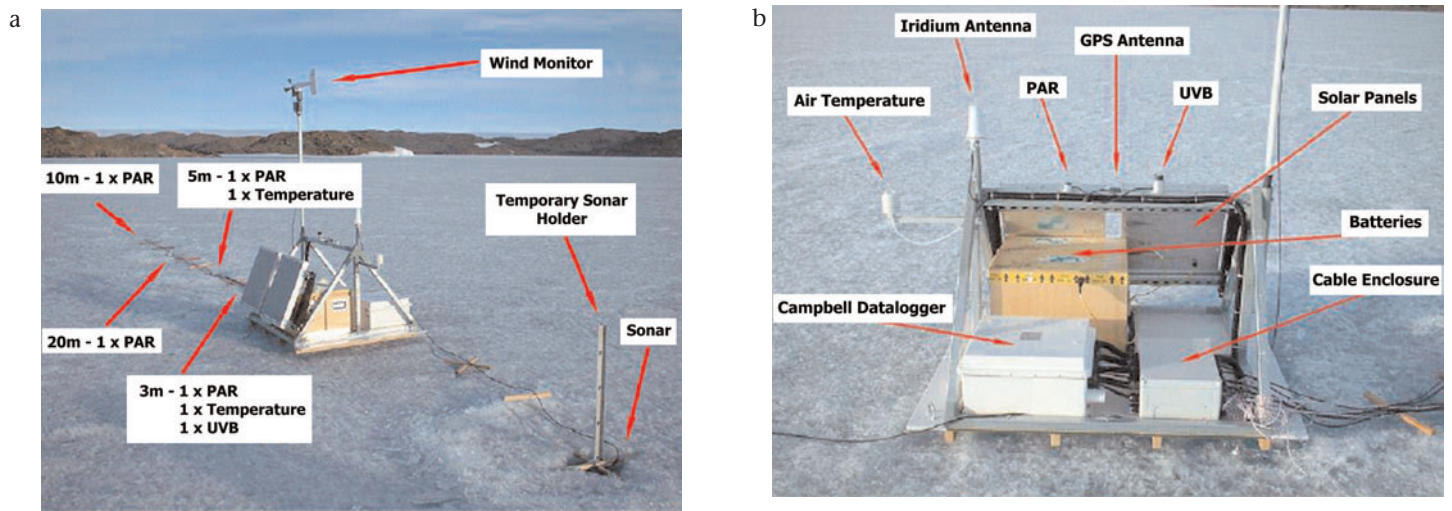


Fig. 2. (a) The remote sensing platform deployed on the ice-cover of Crooked Lake showing the position of PAR, UVB, temperature, wind, and sonar ice thickness sensor. (b) Close-up view of the instrumentation located around the data acquisition unit on the remote sensing platform.

on the DAS for measuring wind speed. Fig. 2a shows the overall layout of the equipment on the lake surface whereas Fig. 2b shows a view of the instrumentation located closely around the data acquisition unit. A complete inventory of all the

equipment deployed on the lake is illustrated in the schematic shown in Fig. 3.

The platform was designed to be rugged with a low center of mass, yet allowing easy access to all the components and

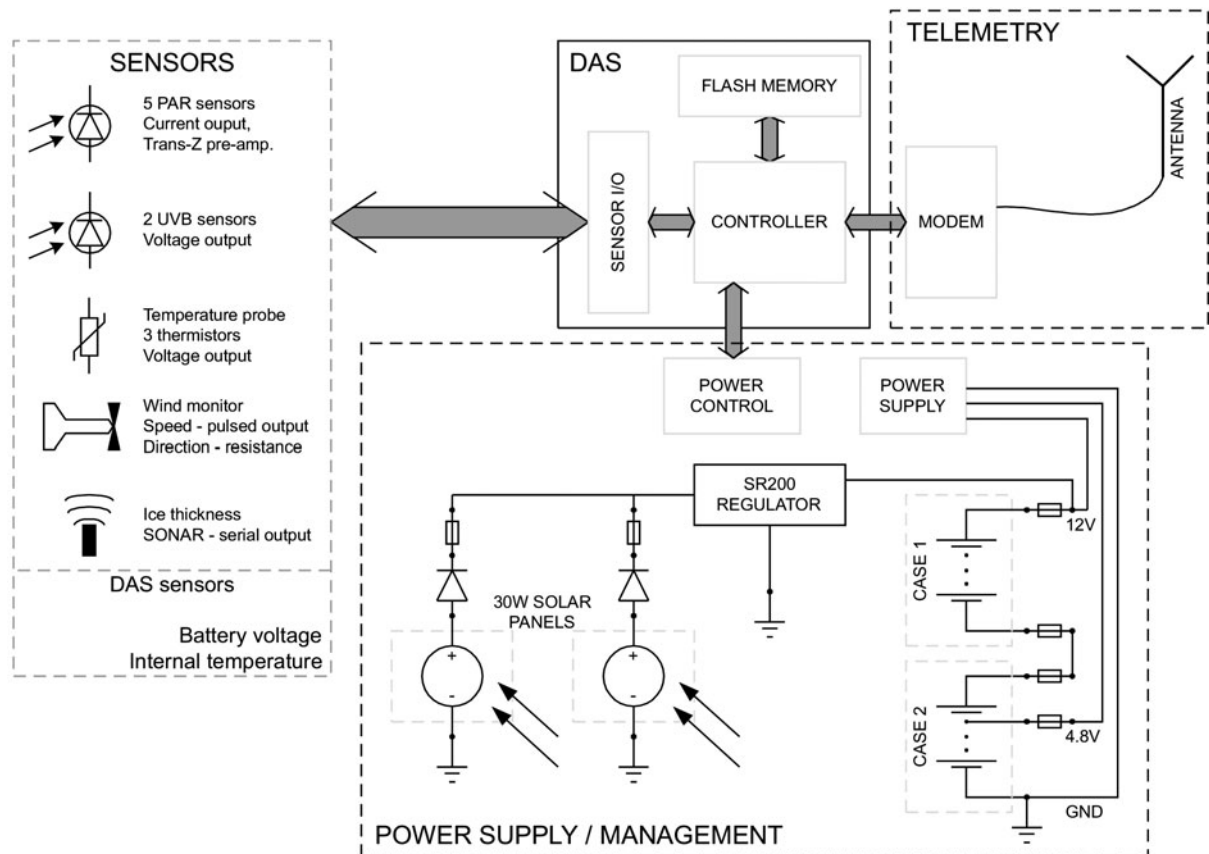


Fig. 3. Diagram showing a complete inventory of all the equipment deployed on Crooked Lake

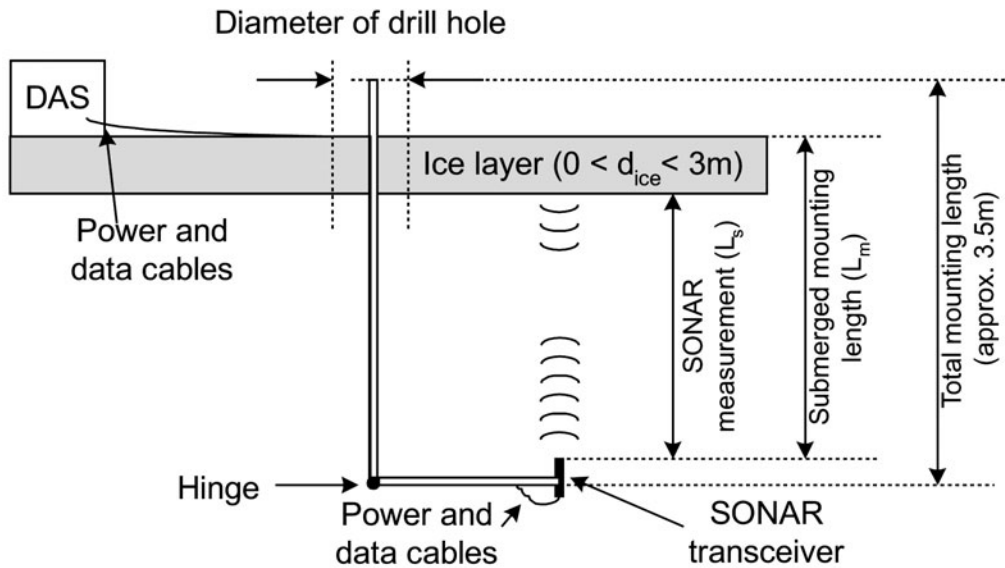


Fig. 4. Diagram of the system used for measuring ice thickness

lifting points. Snowdrift was expected, so measures were taken to avoid ingress into various enclosures. The base had to possess a good thermal insulation to avoid the equipment warming and melting into the ice surface during summer.

A Campbell Scientific datalogger (CR10X) was used, and this determined the choice of a number of the sensors, which were also manufactured by Campbell Scientific, thereby allowing ease of integration.

Details of the sensors are as follows:

Ice thickness measurement. We examined a number of options for accurately measuring ice thickness. One option was a high-cost system that required a component to be anchored to the lake bed. We opted for a simple less expensive system that operated solely from just below the ice. An upward-looking SONAR altimeter was used to measure ice thickness at the point of installation. Fig. 4 illustrates the sensor position in normal operation. The ice thickness, d_{ice} , is calculated from the distance measured underwater by the SONAR transceiver, L_s , and the fixed length, L_m , measured at installation:

$$d_{ice} = L_m - L_s.$$

A Tritech PA500/6 SONAR precision altimeter was used for the underwater SONAR distance measurement. This device normally is used by submarines to measure height above seabed. On activation the transducer sends a 500-kHz ultrasonic signal with a 6° conical beam width. The unit calculates the distance from the first return time signal of the emitted

ultrasonic pulse with a resolution of 1 mm and accuracy of ± 2.5 mm. This transducer has a measurement range of between 0.1 m and 50 m.

The altimeter unit was powered from a 12V supply controlled by the DAS. It was powered only for a short period prior to the measurement and then immediately switched off afterward to save power. The total powered time per sample was approximately 10 s. Communication between the DAS and the altimeter was by a 3-wire RS232 serial cable. The device was triggered by sending a single ASCII character that acted as a command to execute a single measurement. On completion of the distance measurement the altimeter returned the distance in ASCII format.

The altimeter was mounted on an aluminum mounting that became permanently frozen into the ice. A hinged mounting was required as indicated in Fig. 4 so that the SONAR apparatus could fit through the 250-mm-diameter hole created by drilling. At deployment, the hinged system allowed the sensor to deploy at right angles (Fig. 4).

PAR measurement. Our past experience of measuring PAR in polar lakes has demonstrated the reliability of LI-COR instruments in these extreme environments. They are robust and relatively inexpensive. Consequently four LI-COR LI-192SA Quantum Spherical light sensors were used to measure PAR underwater at depths of 3 m, 5 m, 10 m, and 20 m. A single LI-190SA Quantum sensor was used to measure the incident value on the surface. They are solid-state sensors with an optical filter. They produce a current proportional to the incident light intensity at wavelengths between 400 nm and 700 nm. Transimpedance amplifiers were designed to convert the cur-

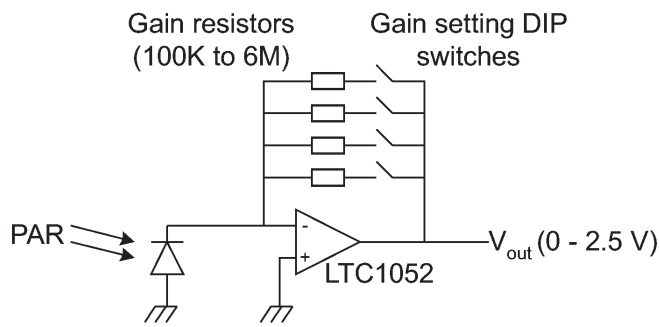


Fig. 5. Transimpedance amplifier for each PAR channel

rent output to a voltage suitable for the A/D acquisition circuitry of the DAS. Fig. 5 shows the transimpedance amplifier circuit implemented for each of the five channels.

To accommodate a wide range of light levels in each PAR sensor various gain settings were available for each channel by switching in different combinations of resistors. The gain settings varied between 100KΩ for the surface sensors to 6MΩ for the underwater sensor at 20 m depth. These were chosen at the time of installation. At this time, zero offset values, V_{offset} , were also measured at the amplifier outputs. The amplifiers LTC1052C, having a lower operating temperature range of -40°C , were mounted on printed circuit boards and installed inside the DAS enclosure.

The light level measured by each channel was measured in terms of the number of incident quanta per unit area and per unit time, the units being $\mu\text{mol s}^{-1} \text{m}^{-2}$. To calculate the PAR measured by each sensor the equation below was applied:

$$\text{PAR} = (1 \times 10^9 / C_n G_n) (V_{out} - V_{offset})$$

where, for each channel, G_n is the gain setting, C_n is the PAR calibration constant (of dimensions $\mu\text{A per } \mu\text{mol s}^{-1} \text{m}^{-2}$), V_{out} is the output voltage for the circuit in Fig. 5, and V_{offset} is the output voltage with zero incident PAR. The combination of the PAR sensor and the transimpedance amplifier resulted in a measurement accuracy of approximately $\pm 0.5 \mu\text{mol s}^{-1} \text{m}^{-2}$.

Table 1. Data output

Sensor	Type	Number	Total Data (Bytes/sample)	Data per day (Bytes)
Sonar altimeter	Tritech PA500/6	1	2	576
PAR light sensors	LICOR LI-192SA/190SA	5	10	2880
UVB light sensors	Skye SKU-430	2	4	1152
Thermistor probes	Campbell Scientific 107	3	6	1728
Wind speed	RM Young Wind Monitor	1	2	576
Wind direction	RM Young Wind Monitor	1	2	576
Battery voltage	CS CR10X	1	2	576
Internal temperature	CS CR10X	1	2	576
Housekeeping data		5	10	2880
Total			40	11.25K

UVB radiation measurement. Skye Instruments SKU-430 UVB sensors were used to measure UVB radiation between 280 nm and 315 nm, both above and below the ice layer. They were selected because they were reasonably priced, available within our time scales, and had guaranteed performance under water. These sensors were powered from a 5V supply controlled by the DAS. Power was applied for a short period before sampling times to allow the sensor output to stabilize. The sensor power was switched off immediately after the sampling instant. A calibrated voltage output of $150 \text{ mV W}^{-1} \text{m}^{-2}$ was provided between 0 V to 1 V, directly proportional to the incident light level. The sensor outputs were connected to the DAS inputs as no further signal conditioning was required. This sensor, when combined with the DAS, provides a UVB measurement with an accuracy of better than $\pm 5 \text{ mW m}^{-2}$.

Temperature measurement. Campbell Scientific 107 Temperature Probes were used for all temperature measurements and deployed at 3 m and 5 m in the water column under the ice. As indicated above they were selected because they were easily integrated with the datalogger, also manufactured by Campbell Scientific. In addition an air temperature sensor was mounted on the equipment mainframe. The probes use a single thermistor with precision resistors mounted within the probe and provide an accuracy of $\pm 0.1^{\circ}\text{C}$ down to -20°C when the correct measurement procedure is implemented. This procedure is incorporated within the datalogger standard functionality and involves an AC excitation of the thermistor and calculates the temperature using a fifth-order polynomial fitting routine (Campbell Scientific 2002).

Wind measurement. A combined direction and speed sensor was used (RM Young Wind Monitor). These were also easily integrated with a Campbell Instruments datalogger. Direction was measured from the resistance of a potentiometer on the monitor mounting shaft whereas the speed was calculated by counting pulses using the DAS from the output of the generator connected to the propeller shaft.

Table 1 tabulates the quantity of data output expected from each of the sensors assuming a 5-min sampling interval.

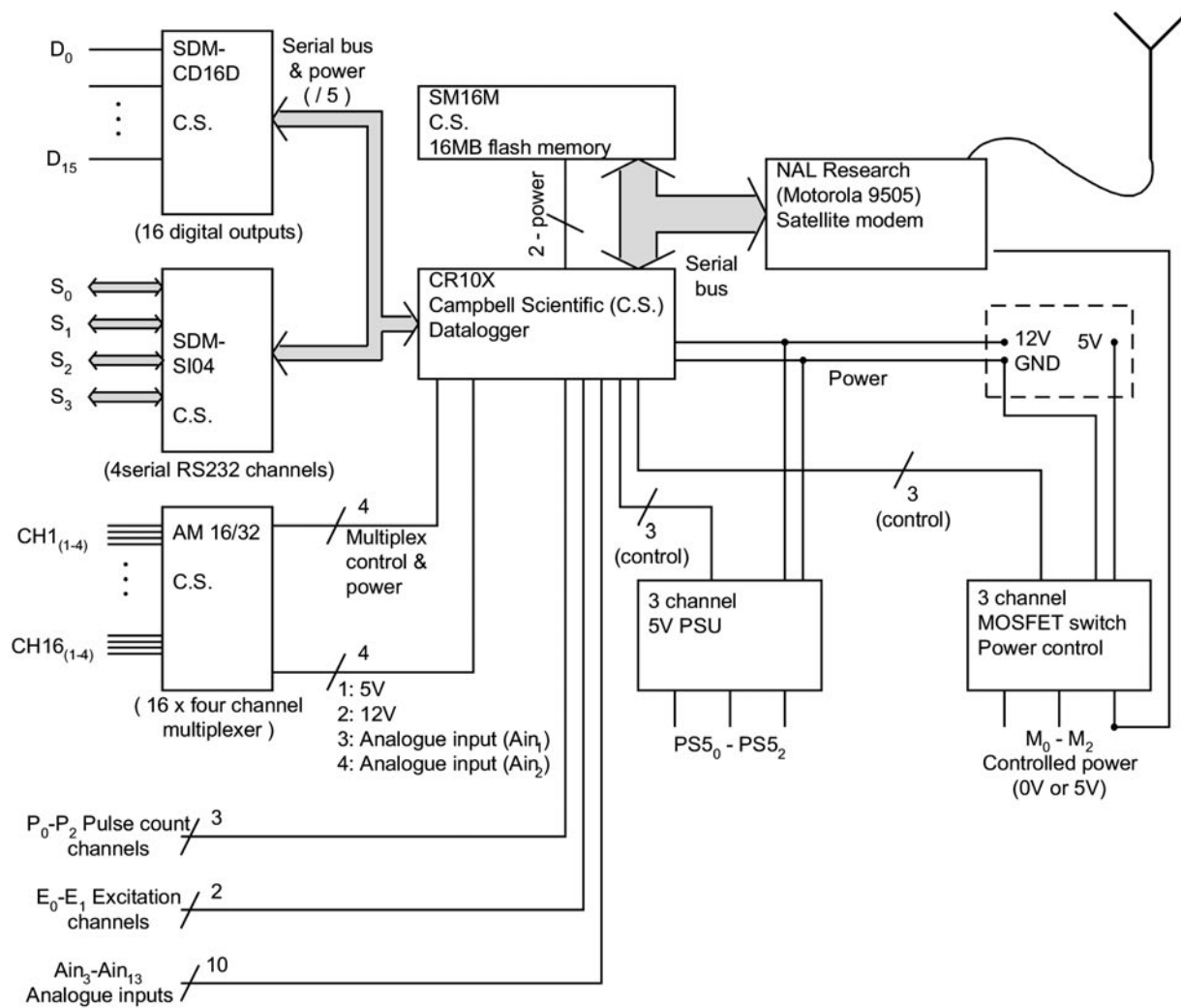


Fig. 6. Data acquisition, telemetry, and power management components

Data acquisition system—The DAS used was based around a modular, commercially available system. Fig. 6 shows the components of the DAS. The DAS is centrally controlled by a datalogger (CR10X, Campbell Scientific). This unit is based upon a Hitachi microcontroller. The system was chosen for proven reliability, flexibility, low power consumption, and low temperature operation (specified to -55°C). The manufacturer offers the equipment with an extended temperature range of -50°C to $+50^{\circ}\text{C}$. These specialized versions are tested for periods in test chambers prior to supply. The peripheral components shown gave the system greater sensor connectivity and some redundancy in case of partial failure. This was achieved through the addition of the AM16/32 multiplexer and the SDM-SI04 serial I/O interface, allowing an increased number of sensors to be connected to the datalogger.

Data were recorded from all the sensors described at a 5-min sampling interval. Additionally the internal datalogger temperature, the battery voltage and a number of variables

recording any communication failures were recorded. Sampled data were initially stored in volatile memory and automatically copied to nonvolatile flash memory for long-term storage, provided by a removable Campbell flash memory module (16 Mb giving 1000 d of storage; Part nr SM16M). In the event of a telemetry failure the sampled data could be manually downloaded from the flash memory by visiting personnel when convenient. The flash memory (SM16M storage module; Campbell Scientific) was capable of storing sampled data for well over a year before overwriting previously stored data.

Telemetry—Three transmission systems were considered for the wireless telemetering of data to Davis Station some 15 km from Crooked Lake. These were VHF radio, HF radio, and satellite telephone. The terrain of the Vestfold Hills was unsuitable for VHF radio without the installation of a repeater station. HF radio was ruled out because of poor rates of data transmission and high current consumption. Therefore a satellite telephone

system was chosen. There are a number of providers that cover parts of Antarctica including Argos, Inmarsat, and Iridium. Iridium was selected because it provides worldwide coverage via a constellation of low earth-orbiting satellites. Consequently the power needed to transmit data to a satellite is much lower than for networks that employ geostationary satellites, such as Inmarsat.

The Iridium system was comprised of an antenna mounted to the frame and the modem unit, a NAL Research Motorola 9505. The modem was connected to the DAS through a serial RS232 connection with communication using standard Hayes commands. The Iridium antenna can be seen in Fig. 2b mounted on top of the steel frame.

The modem was powered from the 4.8V supply (see *Power supply and management*), controlled via the DAS. During transmission the modem current could rise as high as 2A, providing the largest drain on the power resources. To reduce the power consumption of the system, the modem was only energized for 1 h per day—the “communication interval.” Although the bandwidth was limited to 2400 baud, poor reception meant that the actual data rate between the DAS and the host PC was often limited to around 1000 baud.

Communication between the DAS and the host PC could be instigated from either partner during the communication interval. In normal operation, the host PC was programmed to contact the DAS at the start of the communication interval. After the data retrieval was completed the call was terminated and the modem automatically switched off to conserve battery capacity. During this call it was also possible to download a new program to the DAS and, therefore, alter the types of measurement or even the sampling frequency.

Power supply and management—The power system consisted of solar panels for power generation, batteries for energy storage, and circuitry for battery voltage regulation and monitoring. Two Solarex 30W solar panels were chosen to provide power generation for the remote facility due to their inherent reliability and robustness. Manufacturer’s tests included repetitive cycling between -40°C and 85°C , simulated impact of 25 mm hail at terminal velocity and static loading, back of 2400 Pa and front of 5400 Pa. To maintain sufficient power throughout the period of darkness in the winter, a sufficiently large capacity battery was required, and power consumption of all equipment was minimized by providing power to each piece of equipment for the minimum duration possible. The system was designed to operate for 100 d with unaffected performance without any charging from the solar array. In the event of solar panel or regulator failure, this would allow personnel this amount of time to reach the equipment to repair or replace faulty units without any loss of data.

An alternative was to use a small wind turbine. Due to the harsh winter conditions and gusting winds reaching speeds of over 200 km h^{-1} this method was rejected. A possible advantage of a wind turbine would have been that a much smaller battery capacity could have been used as charging would

occur throughout the year. Although in the event of generation failure a small battery capacity would allow less time for personnel to reach the site before data sampling failed.

A 214Ah 12V NiCd industrial battery unit, consisting of 10 Saft SUN-21 1.2V cells in series, was used to power the equipment deployed at the site. This was comprised of two 6V units, 5 SUN-21 cells, each mounted in wooden containers with further insulation and protection. A further connection was provided from one of the containers at 4.8V to be used where appropriate. The containers were protected from the harsh environment although they were not sealed as the battery cells required venting. The particular battery type was chosen for its reliability, robustness, operation at low temperature, and suitability for charging by photovoltaic cells. Any battery that meets these criteria can be used. The batteries must be able to cope with variation in the rate of charging throughout the operation period. The nominal capacity of 214Ah assumes an ambient temperature of 25°C ; at lower temperatures the capacity falls, although this decrease is much less than for lead-acid cells. For example, at -20°C the capacity is only reduced to 160Ah. Operation was also guaranteed in operating temperatures as low as -50°C .

The solar panels were connected in parallel to provide further robustness to failure. They were both mounted to face north to maximize generation during the winter months. A mounting angle of 80° was used as appropriate for the latitude and to minimize the amount of snow settling on the panels. A simple switching regulator, the Rutland SR200, was used to control battery charging. Above a certain battery voltage charging was stopped and excess power dissipated through power resistors mounted in the main datalogger enclosure.

Table 2 shows the average power consumption of the different system components during normal operation, both in active and quiescent modes. The total demand was estimated to be 620 mAh d^{-1} . Without battery charging a theoretical period of autonomous operation lasting 345 d was possible. This period was calculated assuming that the batteries were initially fully charged and the ambient temperature was 25°C . However, at an ambient temperature of -20°C , this period would be reduced to a maximum of 230 d well above the target specification of 100 d, thereby providing an ample safety margin.

Networking—As previously stated, data telemetry was achieved using the Iridium satellite network connection. The connection to this network could in fact be made via any standard phone connection as well as with the dedicated hardware previously described. Consequently the host PC may be situated anywhere with access to a phone connection with international dialing. However, in this work the host PC at Davis station was equipped with identical equipment as installed at the lake site. This configuration, shown in Fig. 1, was chosen because call charges were reduced when the call was kept within the satellite phone provider’s own network. Obviously

Table 2. Power requirements

Equipment/Sensor	Current (mA)		Usage (min d ⁻¹)	Quantity	Daily demand (mAh d ⁻¹)
	Active	Quiescent			
CR10X datalogger	46	1	144	1	132
SM16M storage module	50	0.2	29	1	29
SDM-SI04 serial interface	30	0.7	48	1	40
SDM-CD16D digital outputs	0.1	0.1	144	1	2
AM419 relay multiplexer	17	0.1	86	1	27
Modem (transmitting)	400	0	5	1	35
Modem (receiving)	60	0	60	1	60
SONAR depth altimeter	160	0	48	1	128
PAR light sensors	12	0	30	6	36
UVB light sensors	2	0	20	2	2
Thermistor probe	0	0	60	3	0
Wind speed	0	0	60	1	0
Wind direction	0	0	60	1	0
Battery self-discharge	0	*	0	1	128
Total					619

*Estimated from manufacturer's specification

the host PC was also situated at Davis station during this work for convenience and testing purposes.

The host PC was TCP/IP networked to the station LAN and to the Internet via the station's own satellite communications link to the rest of the world, ANARESAT. As a result, remote access to data was possible by researchers at Nottingham with Internet access. For security reasons, the data were mirrored on an external Web site and not accessed directly from the host PC. Direct connection to the DAS was still possible using the standard phone connection described previously.

Quality control—At regular intervals visits to the site enabled checks on the equipment sensors using other compatible sensors for air temperature, PAR, wind speed and direction, water temperature, and ice thickness. These tests showed compatible data.

Assessment and discussion

The platform was initially deployed for 2 weeks beginning 17 January 2003. This coincided with ice melt-out. The equipment was removed just prior to ice-breakout (1 February 2003) and redeployed after the lake refroze on 12 May 2003 for the winter. During the summer, the battery voltage maintained a high level from solar charging. After winter redeployment, depletion of battery power occurred, with brief phases of recharging. Nonetheless, the batteries maintained sufficient power throughout the phase of winter darkness to enable data acquisition every 5 min.

During summer melt-out, the ice showed a progressive thinning with more rapid thinning just prior to the removal of the platform (Fig. 7a). There were evident small melting and refreezing events during the overall thinning pattern,

and these became much more pronounced as melt increased and the lake formed a moat. During the last 4 d of deployment, there was a large moat around the lake ice-cover, allowing turbulent mixing of colder water that had been in contact with the atmosphere to extend under the ice (Fig. 8a and 8b). Water temperature decreased and showed greater fluctuation. This, combined with a period of strong winds, may have contributed to the apparent melting and refreezing events (Fig. 7a). The platform was redeployed when the ice was 80 cm thick, and during the subsequent days the ice showed a linear pattern of increasing thickness (Fig. 7b). The maximum winter ice cover depth was 2 m. Temperature at the surface and in the water column showed clear diurnal patterns as expected (Fig. 8b).

It should be noted that during winter there was minimal ablation and sublimation from the ice surface and, consequently, the ice thickness measurements were accurate to 5 cm. During summer melt, however, there is likely to be significant ablation, and this would affect the accuracy of the measurements. Consequently the data should be regarded as indicating a trend.

In a modeling context the data from this probe is very valuable for the development, optimization, and validation of theoretical models. The atmospheric variables provide the necessary inputs for models of ice thermodynamics to calculate ice thickness and temperature, which can, in turn, be compared to the data for model validation. On establishing a good correlation between photosynthesis and PAR, it is also possible to couple such physical models with biological models of carbon cycling, where the principal driving force is carbon fixation by phytoplankton. The physical probe data are thus providing

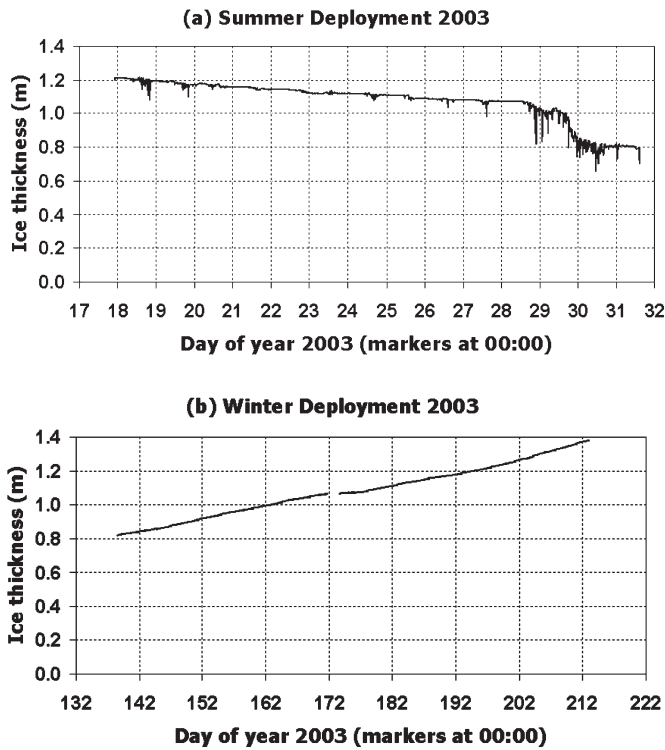


Fig. 7. Ice thickness measurements during (a) summer deployment 17 to 31 January 2003, and (b) winter deployment 12 May to 31 July 2003. Data acquired every 5 minutes.

insight into the functioning of the plankton ecosystem, at times when manual sampling is not possible.

Data taken at 5-min intervals provides a very detailed record of PAR (and UVB levels) in the water column over each day (Fig. 9a and 9b). The examples shown are for two summer

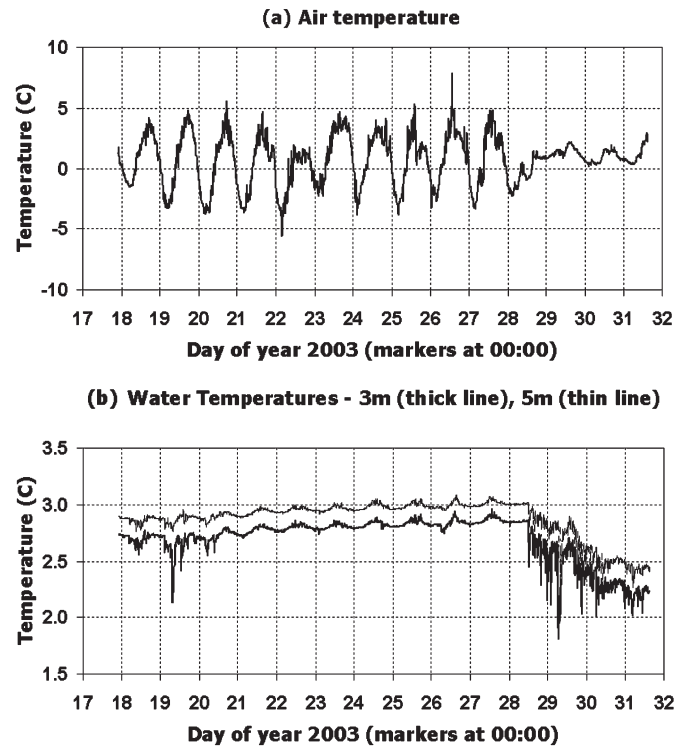


Fig. 8. Temperature in (a) the air or (b) the water column at 3 and 5 m depth, during the period of summer deployment (17 to 31 January 2003). Data acquired every 5 min.

days when the sun did not drop beneath the horizon. One example is for a cloudless day (Fig. 9a), and the other is for a day with intermittent cloud cover (Fig. 9b). Depressions in PAR coincided with intervals when cloud covered the sun. From these data, it is possible to calculate the total light

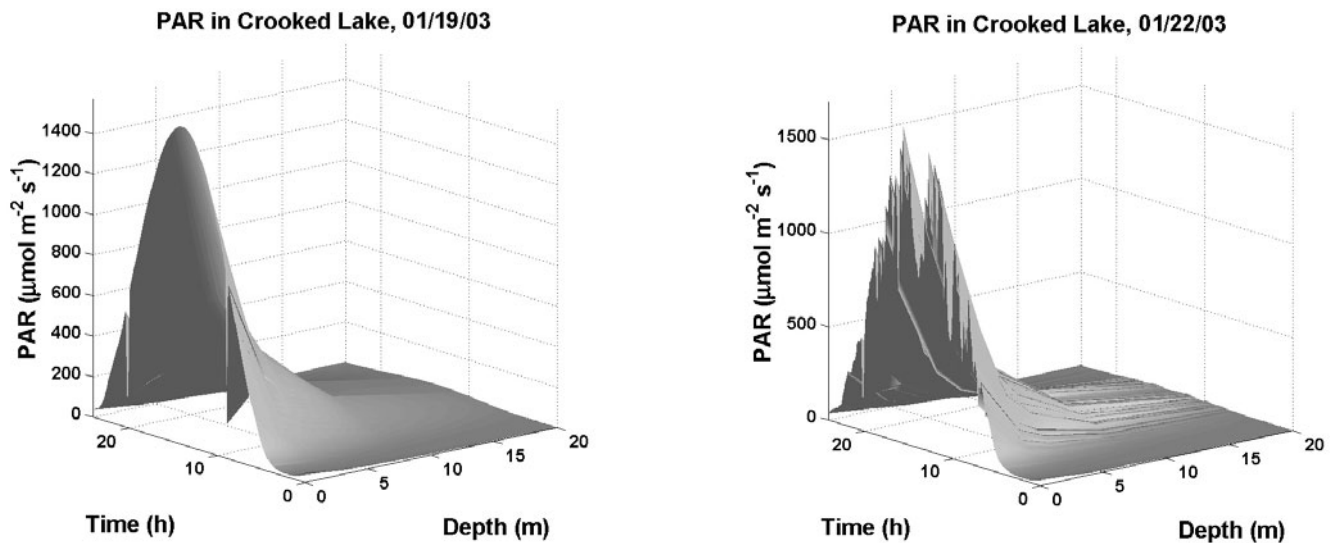


Fig. 9. Photosynthetically active radiation (PAR) for 2 d in the summer period: (a) a sunny cloudless day and (b) a day with intermittent cloud cover. Data acquired every 5 min.

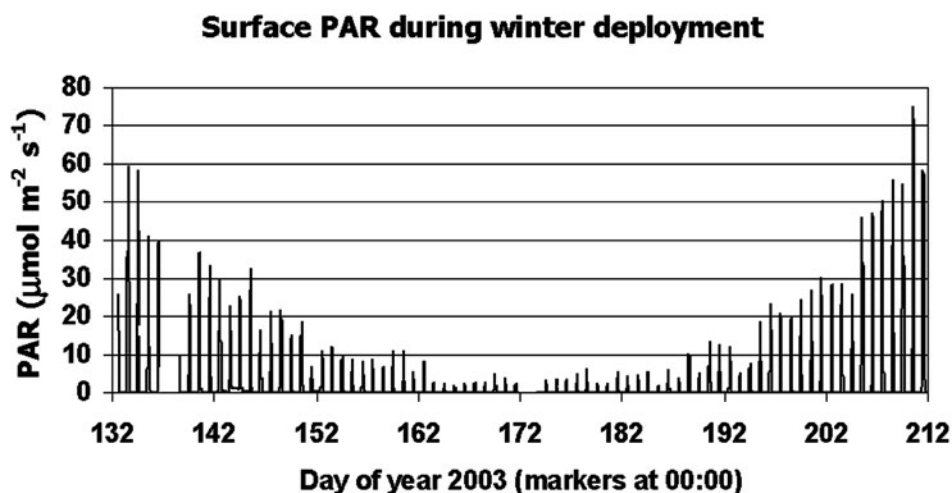


Fig. 10. Surface PAR during the period of winter deployment (period 12 May until 31 July 2003). Peaks coincide with midday.

energy entering the water column on each day. In Fig. 9a (a sunny day), it was 61.8 mol m^{-2} , and in Fig. 9b (a cloudy day) it was 53.1 mol m^{-2} . The maximum compensation depth (depth at which PAR is 1% of the value reaching the ice surface) on these days was calculated to be 22.85 m and 21.44 m respectively (by fitting a Beer's Law exponential curve to the underwater PAR data). There is the potential with such detailed data acquisition, to conduct in situ primary production experiments that can be related directly to accurate light energy levels. Moreover, the frequency of PAR data acquisition can be increased to 1-min intervals if required for experimental purposes. Previous work on Crooked Lake has shown that photosynthesis starts as soon as the phase of winter darkness ends, at a time when inorganic nutrients (nitrogen and phosphorus) are not limiting (Bayliss et al. 1997; Henshaw and Laybourn-Parry 2002). At such times it is the availability of light that limits the rates of photosynthesis. Having accurate values for the levels of PAR available in the water column in relation to rates of carbon fixation at such times has the potential to provide a more detailed understanding of phytoplankton physiology in these extreme lake ecosystems. In summer, it is inorganic nutrient availability that limits carbon fixation by the phytoplankton. There is evidence of surface inhibition in summer (Bayliss et al. 1997). Having fine detail, time-related data on PAR in the water column has the potential to allow a detailed investigation into this phenomenon. Data acquired every 5 min can also be used to provide a broader picture of PAR as shown in Fig. 10, which covers the phase of mid-winter darkness.

Error analysis was conducted to determine the effects caused by extremes of temperature and long-term drift of sensor calibration. The analysis was applied to the PAR sensor deployed at 3 m below the ice surface and the UVB sensor on the main equipment frame. Temperature affects the measurement of PAR in a number of ways. The PAR sensors are cali-

brated at 20°C and for every degree above and below, there is a maximum deviation of 0.15%. For example our highest recorded PAR value of $1042.9 \text{ } \mu\text{mol s}^{-1} \text{ m}^{-2}$ results in a calculated maximum error of 3%. The resistors used in the transimpedance amplifier circuits will change resistance with temperature from the nominal value, which is used to calculate the PAR. Precision resistors are used with a temperature coefficient of resistance of 15 ppm per degree centigrade. The calculated maximum error is 0.03%. The combination of these two errors results in a maximum error of $31.64 \text{ } \mu\text{mol s}^{-1} \text{ m}^{-2}$ or 3.03%.

As no transimpedance amplifier circuits are required for recording of UVB, only the temperature effects on the sensors need to be considered. The sensors have a maximum thermal drift of 0.075 mV per degree centigrade, resulting in an error of 0.64%. Both the PAR and UVB sensors have a maximum long-term drift error of 2%, which results in errors of $20.9 \text{ } \mu\text{mol s}^{-1} \text{ m}^{-2}$ and 0.04 W. The PAR values will also be affected by the changes to V_{offset} of the transimpedance amplifiers. The value will change due to long-term drift and temperature dependence. The calculated errors are negligible at $9 \times 10^{-11}\%$ and $4.6 \times 10^{-10}\%$ for temperature and drift effects respectively.

Long-term surface solar radiation measurements have been made in the McMurdo Dry Valleys since 1993 (Dana et al. 2000). However, the annual data were downloaded manually during summer access to the field sites. This project is therefore unique in presenting the opportunity of being able to provide real-time data from remote sites to any computer in the world.

References

- Bayliss, P., J. C. Ellis-Evans, and J. Laybourn-Parry. 1997. Temporal patterns of primary production in a large ultra-oligotrophic Antarctic freshwater lake. *Polar Biol.* 18:363-370.
- Campbell Scientific Ltd. 2002. CR10X measurement and control module instruction manual. Issued 1/3/02.

- Chapman, W. E., and J. E. Walsh. 1993. Recent variations in sea ice and air temperatures in high latitudes. *Bull. Am. Met. Soc.* 74:33-47
- Dana, G. L., R. A. Wharton, and R. Dubayah. 2000. Solar radiation in the McMurdo Dry Valleys, Antarctica, p 39-64. *In* J. C. Priscu (ed.) *Ecosystem dynamics in a polar desert, the McMurdo Dry Valleys, Antarctica*. American Geophysical Union, Antarctic Research Series 72, Washington D.C.
- Doran, P. T., and others. 2002. Antarctic climate cooling and terrestrial ecosystem response. *Nature* 425:517-520.
- Edwards, A. M., and J. Brindley. 1999. Zooplankton mortality and the dynamical behaviour of plankton population models. *Bull. Math. Biol.* 61:303-339
- Fang, X., and H. G. Stefan. 1996. Long-term lake water temperature and ice cover simulations/measurements. *Cold Regions Sci. Tech.* 24:289-304.
- Fritsen, C. H., and J. C. Priscu. 1999. Seasonal change in the optical properties of the permanent ice cover on Lake Bonney, Antarctica: consequences for lake productivity and phytoplankton dynamics. *Limnol. Oceanogr.* 44:447-454.
- Henshaw, T., and J. Laybourn-Parry. 2002. The annual patterns of photosynthesis in two large, freshwater, ultra-oligotrophic Antarctic lakes. *Polar Biol.* 25:744-752.
- Launiainen, J., and B. Cheng. 1998. Modeling of ice thermodynamics in natural water bodies. *Cold Regions Sci. Tech.* 27:153-178.
- Laybourn-Parry, J. 1997. The microbial loop in Antarctic lakes, p 231-240. *In* C. Howard-Williams, W. Lyons, and I. Hawes (eds.) *ecosystem processes in Antarctic ice-free landscapes*. A.A. Balkema/Rotterdam/Brookfield.
- Lyons, W. B., L. R. Bartek, P. A. Mayewski, and P. T. Doran. 1997. Climate history of the McMurdo Dry Valleys since the last glacial maximum: a synthesis, p 15-22. *In* W. B. Lyons, C. Howard-Williams, and I. Hawes (eds.) *Ecosystem processes in Antarctic ice-free landscapes*. A. A. Balkema/Rotterdam/Brookfield.
- Marshall, W., and J. Laybourn-Parry. 2002. The balance between photosynthesis and grazing in Antarctic mixotrophic cryptophytes. *Freshwater Biol.* 47:2060-2070.
- Peeters, F., D. M. Livingstone, G. H. Goudsmit, R. Kipfer, and R. Forster. 2002. Modeling 50 years of historical temperature profiles in a large central European lake. *Limnol. Oceanogr.* 47:186-197.
- Roberts, E. C., J. Laybourn-Parry, D. M. McKnight, and G. Novarino. 2000. Stratification and dynamics of microbial loop communities in Lake Fryxell, Antarctica. *Freshwater Biol.* 44:649-662.
- Sverdrup, K. A., A. C. Duxbury, and A. B. Duxbury. 2003. *An introduction to the world's oceans*. McCraw-Hill.
- Steele, J. H., and E. W. Henderson. 1981. A simple plankton model. *Am. Nat.* 117:676-691.
- Webster, J., I. Hawes, M. Downes, M. Timperley, and C. Howard-Williams. 1996. Evidence for regional climate change in the recent evolution of a high latitude pro-glacial lake. *Antarctic Sci.* 8:49-59.

Submitted 24 September 2003

Revised 5 December 2003

Accepted 24 March 2004